

G. Mönch
G. Ilgenfritz

Percolation in alkyl polyglycoside microemulsions

Received: 27 July 1999
Accepted: 8 February 2000

G. Mönch (✉) · G. Ilgenfritz
Institut für Physikalische Chemie
Universität zu Köln
Luxemburger Strasse 116
50939 Cologne, Germany
e-mail: Gerhard.Moench@uni-koeln.de

Abstract Mixtures of oil, water, alkyl polyglycosides and long-chain alcohols form almost-temperature-invariant microemulsions. The phase behaviour depends on the content of cosurfactant, usually long-chain alcohols. We show that the system $C_{8/10}G_{1.5}$ /octane/water/octanol exhibits cosurfactant-induced percolation phenomena. The percolation transition from an electrically conducting oil-in-water microemulsion to an electrically non-conducting water-in-oil microemulsion with increasing cosurfactant content is

observed by measurements of electrical conductivity and time-resolved electric birefringence. The field-off relaxation time yields information on the internal length scale. The scaling behaviour of field-off relaxation times and Kerr constants with respect to the percolation point leads to insight into the influence of cosurfactant on phase behaviour.

Key words Transient Electric Birefringence · Percolation · Alkyl polyglycosides · Microemulsions · Nanostructures

Introduction

Electric percolation phenomena are well documented for ionic Aerosol-OT (AOT) and nonionic alkyl polyglycol ether (C_iE_j) water-in-oil microemulsions. Percolation can be induced by changing the volume fraction of the conducting aqueous phase or by changing the temperature. It can also be induced by high electric fields. The effect describes a steep transition from an almost-nonconducting solution of water droplets in oil to a highly conducting solution where the aqueous phase forms a system-spanning network. The transition occurs in the L_2 one-phase region on phase inversion from a Winsor II to a Winsor I system. The highly cooperative transition is generally called a percolation transition, since it has been shown, most extensively for the AOT system, that the conductivity curve can be quite well described by the laws of “percolation theory” [1, 2].

Mixtures of oil, water, pure alkyl glucosides (C_nG_i) (Fig. 1) or technical grade alkyl polyglycosides (APG) and long-chain alcohols form almost-temperature-invariant microemulsions. Kahlweit and coworkers [3]

have worked out the phase behaviour of such four-component systems and have shown that they exhibit a 2,3,2 phase inversion with increasing cosurfactant content. This is the well-known phase-inversion-temperature phenomenon from temperature-sensitive microemulsions with C_iE_j /oil/water or Igepal CO520 [2, 4]. It has also been proven for the C_8G_1 /octane/water/octanol [5] and C_8G_1 /octane/water/geraniol systems. It is the aim of the present investigation to examine cosurfactant-induced percolation phenomena in APG microemulsions. We use $C_{8/10}G_{1.5}$ /octane/water/octanol systems, which contain a surfactant of technical grade [6]. We characterise the transition by measurements of electrical conductivity and monitor structural and dynamic properties by time-resolved electrical birefringence measurements (Kerr effect).

Via Kerr constants and field-off relaxation times we observe a distinct growth of the compartment size on approaching the percolation threshold from the droplet region with decreasing cosurfactant content. By interpreting the field-off relaxation times as rotational diffusion times, it is possible to estimate the length scale of the

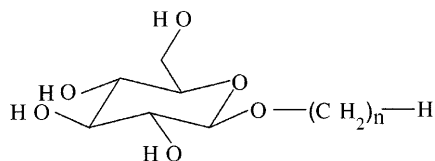


Fig. 1 Structure of $C_{8/10}G_{1.5}$ alkyl polyglycoside (APG). The mean polymerisation degree of glucose is 1.5; n varies from 8 to 10

microstructure. The electric-field-strength dependence of the electrical conductivity will be discussed as field-induced percolation. The marked electric-field dependence of the electrical conductivity demonstrates the possibility of switching this temperature-invariant system from a nonconducting state to a conducting state within several microseconds by applying high electric fields.

Experimental

$C_{8/10}G_{1.5}$ APG 220 UP (Glucopon 215 CSUP), charge number 167 167, was a gift from Henkel and was used without further purification. The APG/water (63.6/36.4) mixture had a pH of 11.9, so no salt addition was necessary for the measurements of the electrical conductivity.

APG/octane/water mixtures were prepared by weighing the components. The titration with octanol was carried out volumetrically using a piston-stroke pipette (Eppendorf Research). Good reproducibility of the phase boundaries is obtained if the APG solution is homogenised for several minutes by vigorous shaking before weighing.

The low-frequency ($\omega = 10^4$ rad/s) electrical conductivity was measured in a thermostated water bath (± 0.05 °C) using a WTW-LTA electrode and a B 331 Wayne-Kerr autobalance precision bridge. For measurements of field effects we used the apparatus described in Refs. [2, 7]. All measurements were carried out at 25 °C.

Results

Phase behaviour and electrical conductivity

The four-component system $C_{8/10}G_{1.5}$ /octane/water/octanol is represented by an isothermal phase tetrahedron at constant pressure (Fig. 2).

Three parameters describe the system:

$$\alpha = m(o)/m(o + w), \quad \gamma = m(s)/m(s + o + w),$$

$$\delta = 100 m(cs)/m(cs + s + o + w), \text{ where}$$

m is the mass, o is oil, w is water, s is surfactant and cs is cosurfactant.

A cut through the phase tetrahedron at constant α produces a triangular plane with a defined oil / water ratio. In this triangular plane the phase boundaries show the characteristic “fish”, the three-phase region forms the body and the one-phase region the tail of the fish. The same phase behaviour is known from the temperature-dependent phase prism of the ternary C_iE_j /oil/water system. Our measurement starts in a plane at

constant $\alpha = 0.7$ with a fixed APG content ($\gamma = 0.15 - 0.30$). With increasing octanol content (increasing δ) the $C_{8/10}G_{1.4}$ /octane/water/octanol system shows a $\bar{2}, L_1, L_\alpha + \text{bicontinuous}, L_2, \bar{2}$ phase sequence (Fig. 3). The L_1 phase is identified as a highly electrically conducting isotropic narrow one-phase region. The adjacent $L_\alpha + \text{bicontinuous}$ two-phase region is characterised by its high electrical conductivity and its birefringence. With increasing δ the optical isotropic L_2 phase is reached. In the L_2 one-phase region a steep decrease in electrical conductivity occurs. Within a narrow range of 1–2% cosurfactant the electrical conductivity drops 2–3 decades.

This “jump” in the electrical conductivity has all the characteristics of a percolation transition known from nonionic and ionic microemulsions induced by increasing and decreasing temperature, respectively. Further addition of octanol leads only to little change in electrical conductivity up to the phase boundary $L_2 \rightarrow \bar{2}$. The microemulsion remains in a low-conducting state, characteristic of a water-in-oil microemulsion, i.e. a solution of water droplets in oil.

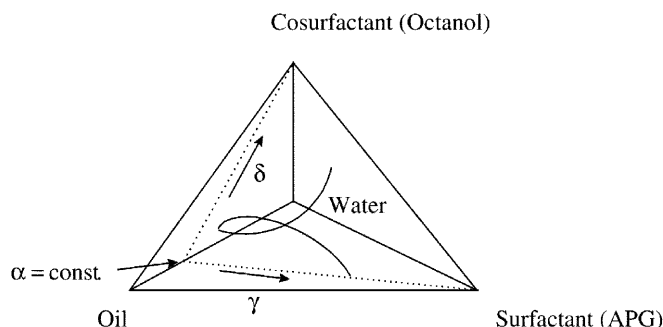


Fig. 2 Schematic isothermal phase tetrahedron of the APG/oil/water/cosurfactant system

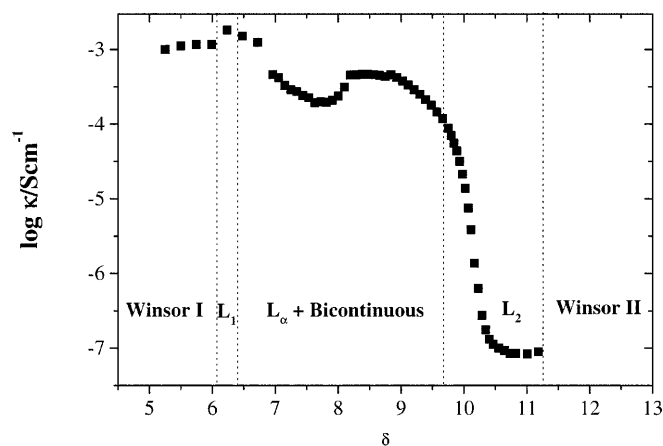


Fig. 3 Electrical conductivity versus cosurfactant content, δ , $\alpha = 0.7$, $\gamma = 0.15$

Lowering γ leads to a shift of the percolation threshold towards smaller δ values (Fig. 4). It is seen from Fig. 4 that the δ dependence of the percolation threshold follows the change in the phase boundary. Again this result parallels the behaviour of C_iE_j , or Igepal, microemulsions if the temperature is used instead for obtaining the phase inversion [4]. A smaller surfactant content (lower γ), i.e. a larger water-to-surfactant ratio, leads to an increase in droplet size and a decrease in the curvature of the amphiphilic film; therefore less cosurfactant is needed for phase inversion.

From the similarities between the influence of temperature and cosurfactant on the phase behaviour of nonionic microemulsions it seems reasonable to apply percolation theory to the measured curves. According to this theory the conductivity of percolating systems

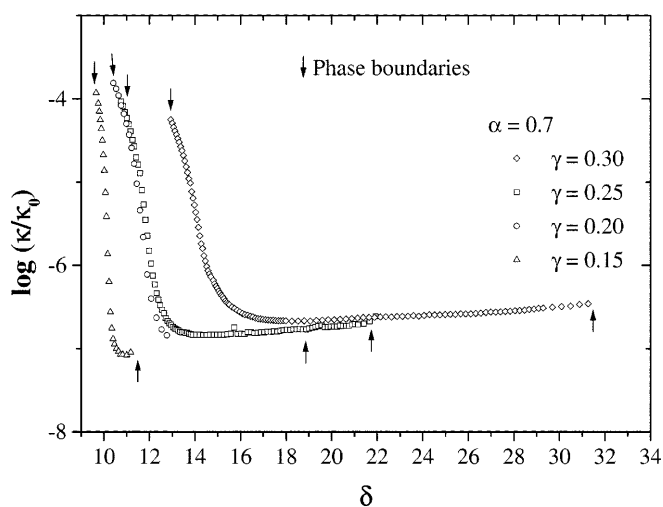


Fig. 4 Electrical conductivity versus cosolvent content, δ , with varying γ

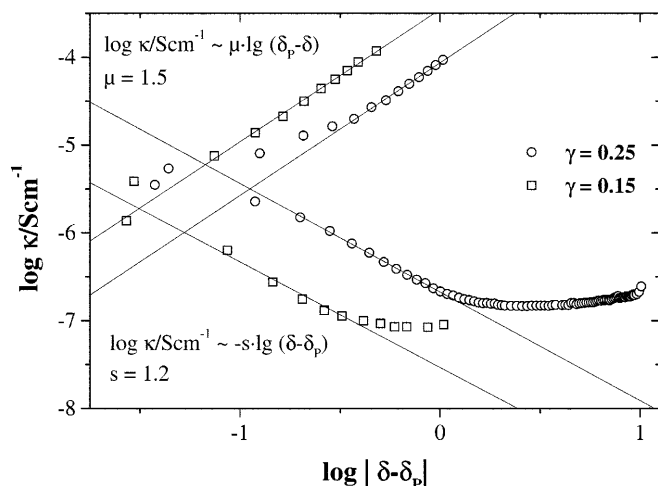


Fig. 5 Electrical conductivity versus $\log(\delta - \delta_p)$ analysis of data in terms of percolation theory

follows universal scaling laws in the vicinity of the transition point, defined as the point where a system-spanning (infinite) cluster of conducting particles form.

Analysis in terms of the scaling laws in the high- and low-conducting region,

$$\log \kappa \sim \mu \log(\delta_p - \delta) \quad \text{for } \delta < \delta_p$$

$$\log \kappa \sim -s \log(\delta - \delta_p) \quad \text{for } \delta > \delta_p,$$

shows that the scaling laws are quite well applicable and lead to exponents of $\mu = 1.5$ and $s = 1.2$ (Fig. 5). Deviations of the exponents from the theoretical values of $\mu = 1.9$ and $s = 1.2$ for dynamic percolation may be due to the difficulties in the fitting procedure.

They may, however, also indicate that the conditions for applying percolation theory are not strictly fulfilled.

Electric birefringence

Examples of the response of the microemulsion system when an electric field pulse is applied are shown in Fig. 6; the changes in the electrical conductivity and birefringence are also shown.

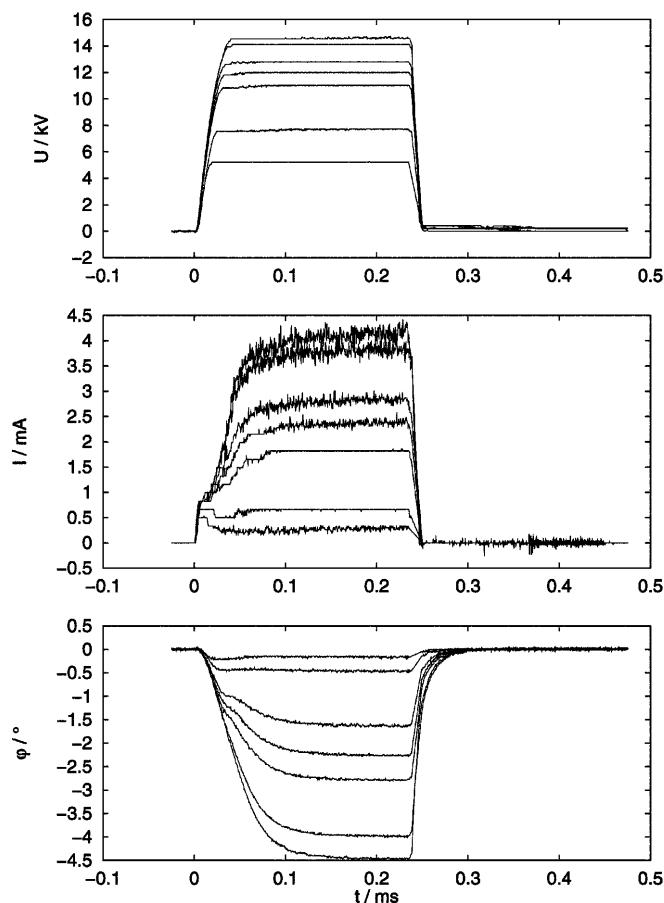


Fig. 6 Time-resolved measurement of phase shift and electrical conductivity ($\alpha = 0.7$, $\gamma = 0.15$, $\delta = 10.9$). The changes in the applied voltage (U), current (I) and phase shift (ϕ) are shown

For lower field strengths an initial fast increase in electrical conductivity and phase shift is detectable. This effect is superimposed by a slower process that reaches a saturation value after 0.1–0.2 ms. The saturation value was used for further analysis of the data.

From the E^2 dependence of the phase shift and the time-resolved conductivity (Fig. 7) two distinct processes are evident. In the droplet region only little changes in the phase shift and the electrical conductivity occur below a critical field strength. On approaching the percolation point the critical field strength decreases. The growth of the phase shift and the electric conductivity above the critical field strength indicates field-induced structural changes. This may be interpreted as clustering of polarised water droplets which at sufficiently high electric fields form an infinite network. All

the APG microemulsions investigated showed a negative electrical birefringence.

In the frame of the Peterlin–Stuart theory [8] this is to be interpreted as an “intrinsic” birefringence of the structural elements, i.e. chains of deformed water droplets. More explicitly, the negative intrinsic birefringence exceeds the possible positive contribution of “form” birefringence. The negative birefringence is consistent with the picture that the elongated water droplets are oriented in the direction of the electric field, the individual surfactant molecules being perpendicular to the prolate structure. Figure 7 shows that in each regime the birefringence is linearly dependent on the square of the field strength, i.e. the Kerr law is fulfilled. The Kerr constants, $B = \varphi/(2\pi l E^2)$, where φ is the birefringence phase shift and l is the light path, are

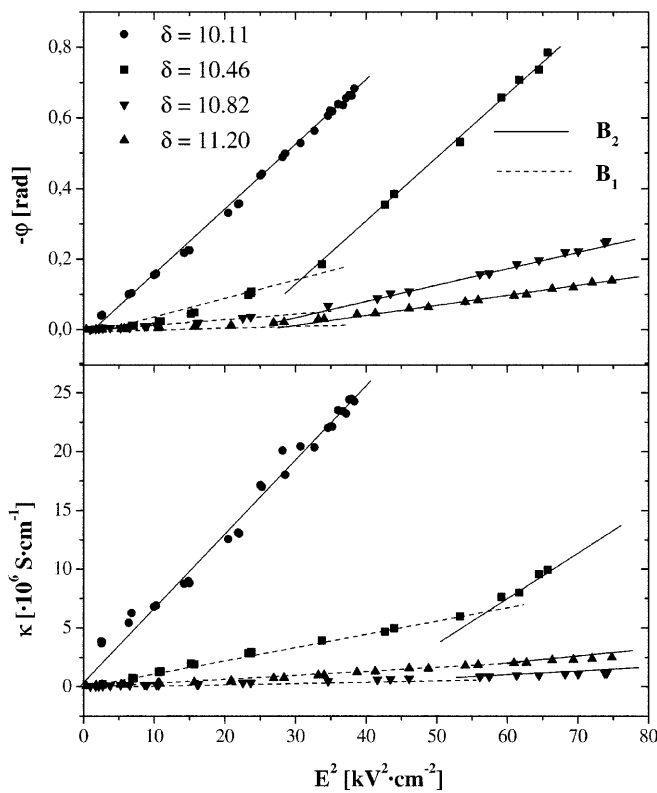


Fig. 7 Phase shift and electrical conductivity versus E^2 ($\alpha = 0.7$, $\gamma = 0.15$)

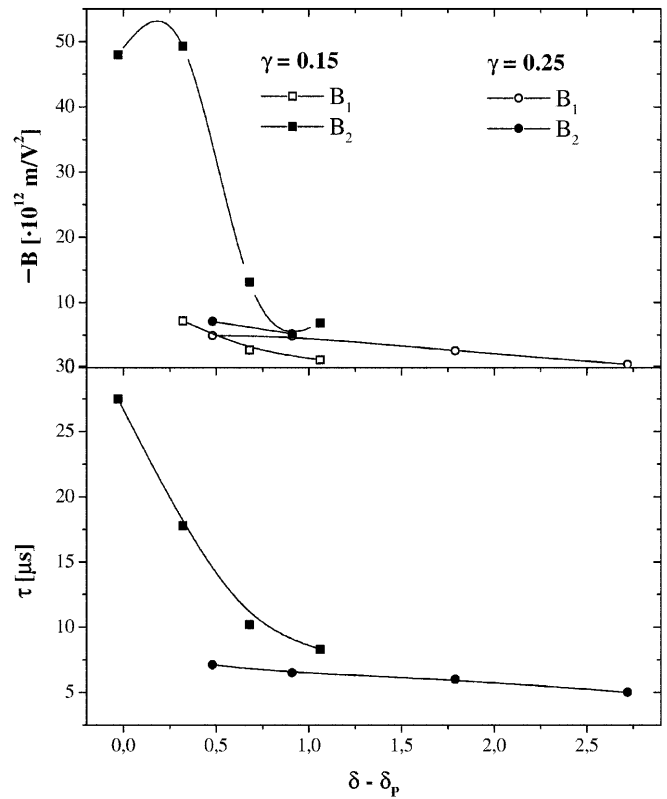


Fig. 8 Kerr constants (B_1 and B_2 -processes) and field-off relaxation times versus δ . $\alpha = 0.7$, $\gamma = 0.15$ (■) and $\gamma = 0.25$ (●)

Table 1 Kerr constants for the B_1 and B_2 (10^{12} m/V²) processes and field-off relaxation times, τ (μ s), for $\alpha = 0.7$ and various γ values

$\gamma = 0.15$				$\gamma = 0.25$			
δ	B_1	B_2	τ	δ	B_1	B_2	τ
10.1		-48	27.5	12.3	-4.9	-7.1	7.1
10.5	-7.2	-49	17.8	12.7	-4.9	-5.2	6.5
10.8	-2.8	-13	10.7	13.6	-2.6		6.0
11.2	-1.2	-6.9	8.3	14.5	-0.5		5.0

obtained from the slope of the curves. In both regimes the values of B_1 ($E < E_{\text{crit}}$) and B_2 ($E > E_{\text{crit}}$) increase by almost an order of magnitude (Table 1). The increase indicates that the droplets are more easily deformed when approaching percolating conditions.

Dynamics

The dynamics of the field-induced aggregation is characteristic of a highly cooperative process: there is a relatively slow formation of the percolating structure in the field, but a rapid disintegration at the end of the pulse (Fig. 6).

Concentrating on the field-off dynamics, it is seen from Fig. 8 that there is a pronounced slowing down when approaching the percolation regime.

It is the distance from the percolation point which determines the magnitude of the Kerr constant, B , and the field-off relaxation time, τ , as is seen from Fig. 8, where the B and τ values are plotted versus the reduced δ values.

The increase in the relaxation times indicates the presence of larger microstructures. For estimates of the correlation length involved we may apply the expression for the rotational relaxation times of a sphere, $\tau = \eta V /$

(kT) , where η is the viscosity and V is the volume of the effective sphere. With the viscosity of octane we obtain effective radii of water droplets/droplet clusters of 20–40 nm.

Conclusions

Percolation studies have so far been performed on ionic and nonionic microemulsions by variation of the amount of conducting phase or of temperature. Temperature-invariant microemulsions with APG exhibit percolation behaviour on phase inversion as a function of cosurfactant content. We have here a system which allows these phenomena to be studied with a new order parameter. Analogous to the influence of temperature, the cosurfactant increases the curvature towards the water droplets.

Percolation can also be induced by high electric fields. Time-resolved measurements of the electric current and of the birefringence give information on the dynamics of the aggregation process of droplets to a system-spanning network. It is shown that the nonconducting system of water droplets in oil can be switched within a few microseconds to a highly conducting solution where the aqueous phase percolates.

References

1. (a) Lagues M, Ober R, Taupin C (1978) *J Phys Lett* 39:487–491; (b) Kim MW, Huang JS (1986) *Phys Rev A* 34:719–722; (c) Stauffer D, Aharony A (1994) *Introduction to percolation theory*, 2nd edn. Taylor & Francis, Bristol
2. Schlicht L, Spilgies J-H, Runge F, Lipgens S, Boye S, Schübel D, Ilgenfritz G (1996) *Biophys Chem* 58:39–52
3. Kahlweit M, Busse G, Faulhaber B (1995) *Langmuir* 11:3382–3387
4. (a) Kahlweit M, Strey R (1985) *Angew Chem* 97:655; (b) Strey R (1994) *Colloid Polym Sci* 272:1005–1019
5. Stubenrauch C, Paepflow B, Findenegg GH (1997) *Langmuir* 13:3652–3658
6. von Rybinski W, Hill KH (1998) *Angew Chem* 110:1394–1412
7. Runge F, Röhl W, Ilgenfritz G (1991) *Ber Bunsenges Phys Chem* 95:485–490
8. Peterlin A, Stuart HA (1939) *Z Phys* 112:129